Peculiar Temporal Structure of the South China Sea Summer Monsoon

Bin Wang ① and *Renguang Wu*
Department of Meteorology, University of Hawaii, USA
Received January 31, 1997

ABSTRACT

Beijing located at the junction of four major components of the Asian–Australia monsoon system (the Indian, the western North Pacific, the East Asian subtropical, and the Indonesian–Australian monsoons), the monsoon climate over the South China Sea (SCS) exhibits some unique features. Evidences are presented in this paper to reveal and document the following *distinctive features* in the temporal structure of the SCS summer monsoon:

(1) pronounced monsoon singularities in the lower tropospheric monsoon flows which include the pre-onset and withdrawal easterly surges and the southwesterly monsoon bursts at Julian pentad 34–35 (June 15–24) and pentad 46–47 (August 14–23);

(2) four prominent subseasonal cycles (alternative occurrences of climatological active and break monsoons);

(3) considerably larger year-to-year variations in convective activity on intraseasonal time scale compared to those over the Bay of Bengal and the Philippine Sea;

(4) the redness of the climatological mean spectrum of precipitation / deep convection on synoptic to intraseasonal time scales in the central SCS;

(5) a remarkable asymmetry in the seasonal transitions between summer and winter monsoons and an extremely abrupt mid-May transition (the outburst of monsoon rain and the sudden switch in the lower troposphere winds from an easterly to a westerly regime);

(6) the bi-modal interannual variation of summer monsoon onset (normal and delayed modes).

In addition, the monsoon rainfall displays enormous east–west gradient over the central SCS. Possible causes for these features are discussed. A number of specific science questions concerning some of the peculiar features are raised for the forthcoming SCS monsoon experiment to address.

Key words: Monsoon over SCS; Subseasonal cycles, Spectrum of precipitation, Bi-modal interannual variation

I. INTRODUCTION

Being surrounded by vast Asian landmass to the north and west and by Philippine and Indonesian archiqelagos to the east and south, the South China Sea (SCS) is located at a unique geographic location–the junction of the three major Northern Hemisphere Summer Monsoon components: the Indian (or South Asia) summer monsoon (ISM), the western North Pacific summer monsoon (WNPSM), and the East Asia Subtropical monsoon (EASM). It also exposes to the influences of equatorial disturbances and connects with Australian winter monsoon through cross-equatorial flows. The complex surface boundary conditions and the unique large-scale environmental setting favor certain specific processes of interaction among land, ocean, and atmosphere which result in some specific features of

①Corresponding author's address: Dr. Bin Wang, Department of Meteorology, University of Hawaii, 2525 Correa Road, Honolulu, Hawaii 96822, USA. <e-mail> bwang@soest.hawaii.edu.

the South China Sea summer monsoon (SCSSM). For instances, as noted by Zhu et al. (1986) and Huang and Tao (1992), the acceleration of the westerly wind component of the SCS monsoon leads that of the easterly counterpart in the Southern Hemisphere (SH) and the change in winds leads the change in moisture field. In contrast, the acceleration of the westerly component of the Indian summer monsoon is nearly synchronous with that of the easterly component in the SH and the change in monsoon winds lags that in moisture field (Krishnamurti, 1985).

Study of SCS monsoon is not only of great interests to regional climate variation but also of importance to undertanding planetary-scale climate variability. From a regional point of view, a better understanding of physical processes governing the evolution of SCSSM and an improved weather and climate prediction have conceivably large positive impacts on socio-economic development in many densely populated neighboring countries. From a global point of view, the convection anomalies associated with SCSSM and WNPSM may interact with basic summertime flows and exert significant influences on the climate anomalies over downstream East China Sea, Japan, and North America (Nitta 1987; Lau and Peng, 1992), and on the monsoon rainfall anomalies over China (Huang and Li, 1988 and many others). The ocean-atmosphere interaction over SCS was speculated as a potential key process in sustaining prominent tropospheric quasi-biennial oscillation (e.g., Tomita and Yasunari, 1996). There are increasing evidences which make the authors believe that the dramatic abrupt transition in mid-May (Matsumoto, 1992; Lau and Yang, 1997) is one of the benchmarks of boreal spring transition of the planetary-scale circulation. This boreal spring transition provides a natural start of the "monsoon year" (Yasunari, 1991) and possibly contributes to the "predictability barrier" for El Nino-Southern Oscillation (ENSO) prediction (Webster and Young 1992).

Largely due to lack of long-term reliable observations over the vast area of SCS, we do not have an adequate background knowledge of the detailed temporal and spatial structures of the SCSSM. We need to be cautious about those conclusions which were inferred from short-term or segregated observations. In order to facilitate planning field experiments for the forthcoming South China Sea Monsoon Experiment (SCSMEX), we have conducted a preliminary study of the temporal structure of the SCS summer monsoon. Specific efforts are made to identify distinctive features of SCS monsoon which pose some curious scientific questions regarding the nature of the processes of the coupled monsoon system.

The next section explains data and analysis procedure adopted in the present study. We then describe premier features of SCSSM in the context of the seasonal march (Section 3), the monsoon singularities (Section 4), the subseasonal cycle (Section 5), the mid-May transition (section 6), the year-to-year variability of intraseasonal oscillation (Section 7), the bi-modal behavior of the interannual variation in SCS summer monsoon onset (Section 8), and the spectral behavior of transient disturbances (Section 9). The last section summarizes fundamental characteristic evolution of the SCSSM and discusses scientific problems for future investigations.

II. DATA AND ANALYSIS PROCEDURE

1. *Datasets*

The present study used three types of data: (I) satellite observations which provide estimates for rainfall and deep convection, (ii) the gridded global analysis by European Centre for Medium Range Weather Forecast (ECMWF), and (iii) the comprehensive ocean-atmos-

phere data set (COADS).

The datasets used to infer tropical convection and rainfall include Outgoing Longwave Radiation (OLR), Highly Reflective Cloud (HRC), and infrared equivalent blackbody temperature (T_{BB}). The pentad mean OLR data were obtained from Climate Prediction Center / National Center for Environmental Prediction (NCEP) on a $2.5 \times 2.5^{\circ}$ grid for a 17-year period from 1975 to 1992 with a nine-month gap in 1978. The HRC data were created by Garcia (1985) by subjectively analyzing daily visible and infrared polar-orbiting satellite mosaics to identify deep, organized convective systems (cloud clusters), which are responsible for most tropical rainfall. The HRC data have a resolution of $1^{\circ} \times 1^{\circ}$ and cover the period from January 1971 to July 1987. The T_{BB} datasets were derived from Japanese's geostationary meteorological satellite with a $1^{\circ} \times 1^{\circ}$ spatial resolution and a three-hour temporal resolution, covering the period of 1980–1993. The ECMWF analysis data set covers a 14-year period from 1979 to 1992. The climatological monthly mean surface winds and sea surface temperature (SST) were computed by Sadler et al. (1987) using COADS for the period of 1900–1979.

Over SCS, monthly mean OLR and Monthly frequency of HRC are well correlated with monthly rainfall. Wang (1994) has summarized statistical relationships among rainfalls, OLR, and HRC derived by Morisse (1986), Motel and Weare (1987), and Kilonsky and Ramage (1976), and suggested the following regression relation: A monthly mean OLR of 240 W / m^2 corresponds to a HRC frequency of three days / month and a rainfall rate of 210 mm / month. Upon this climatological mean relationship, a monthly mean OLR anomaly of 15 W / m^2 corresponds approximately to a HRC anomaly of 1 day / month and a rainfall anomaly of 80 mm / month.

2. *Statistical Significance Test of Climatological Intraseasonal Oscillation (CISO)*

To describe subseasonal variation of mean monsoon, climatological pentad mean data were used. The climatological pentad means $Y_C(I)$ $(I = 1,73)$ can be decomposed into two components: a "smoothed" annual cycle $Y_{AC}(I)$ and a climatological intraseasonal oscillation (CISO) component $Y_{CISO}(I)$. The $Y_{AC}(I)$ is represented by the first three Fourier harmonics (period from 120 days to one year) while the Y_{CISO} is represented by the sum of the 5th–18th harmonics (period from 20 to 72 days). The residual is normally negligible. A question arises as to whether the CISO component is statistically significant from a random noise due to sampling. To address this question, we have taken two types of statistic significance test.

The first test is t-test. The null hypothesis is that the observed sample mean (i.e., the magnitude of CISO) denoted by $ABS(Y_{CISO})$ at a fixed pentad has been drawn from a population characterized by zero mean, i.e., Y_{CISO} is not significantly different from zero. Assume that transient ISOs (with periods of 20–72 days) in each individual years, Y_{ISO} is expressed as the sum of the CISO which is a component phase-locked to annual cycle and a departure from CISO due to year-to-year variation:

$$Y_{ISO}(j) = Y_{CISO} + Y'_{ISO}(j), \quad j = 1,N$$

where N is the number of years over which the climatology was made. The year-to-year variation is measured by sample standard deviation S. Then the test statistic

$$t = ABS(Y_{CISO}) / (S / N^{1/2})$$

follows a student's t-distribution with a degree of freedom of N–1. For given $N = 17$, if $t > 2.12$, the null hypothesis must be rejected at the 95% confidence level, implying that the

CISO cannot be viewed as an ordinary sampling fluctuation, i.e., the amplitude of CISO significantly differs from zero.

The second text examines the null hypothesis that a negative (or positive) sign of transient ISO occurs randomly at any fixed pentad of the calendar year, so that its probability of occurrence is 50%. With this null hypothesis, it can be shown that at any given pentad the probability for 12 or more negative (or positive) anomalies to occur during a 17-year sample would be less than 5%, implying that the null hypothesis must be rejected. Such a pentad is referred to as a wet (dry) singularity, corresponding to a 95% confidence level.

III. CONSPICUOUS ASYMMETRIES IN THE ANNUAL CYCLE

1. *Temporal Asymmetry in Seasonal Transitions*

Figure 1 shows seasonal march of surface winds, SST, and monthly frequency of HRC over SCS along 110°E and 120°E, respectively. The annual reversal of surface wind direction from winter northeasterlies to summer southwesterlies (south of 15°N) or southerlies (north of 15°N) delineates unambiguously summer and winter monsoon seasons.

The seasonal march of SCSSM, however, is distinguished from other regions of the Northern Hemisphere tropical monsoon (e.g. ISM and WNPSM) by *an abrupt establishment of surface southerly regime during May nearly simultaneously over a large latitudinal extent from 3°N to 21°N* (Fig.1). In sharp contrast, the summer monsoon withdrawal (re-establishment of northeasterlies) takes about four months and occurs progressively later southward: in September at the latitudes north of 18°N, in October from 10° to 18°N, in November from 5° to 10°N, and in December south of 5°N.

The simultaneous onset and progressive retreat of the SCSSM are also reflected in the seasonal distribution of convective activity and rainfall as estimated by monthly frequency of HRC. The contour of 3 days per month of HRC shown in Fig. 1 outlines rainy seasons at various latitudes. The rainy season starts nearly simultaneously across the entire latitudinal extent of SCS in late May, following a rapid increase in SST from March to May. Similar to the withdrawal of southerlies, the rainy season ends progressively later equatorward, more or less in accord with the re-establishment of the northeasterly winter monsoon.

As a consequence of the temporal asymmetry in the seasonal transition, the duration of summer monsoon season increases equatorward from four months in the northmost SCS to 7 months at its southmost latitudes. The peak (strongest) summer monsoon occurs in July north of 15°N and in August south of 15°N.

2. *East-west Contrast and Latitudinal Difference in Monsoon Rainfall*

The seasonal distribution of rainfall exhibits remarkable dissimilarities between the east (along 110°E) and west (120°E) SCS, although the seasonal march of surface winds shows little difference (Figs. 1a and 1b). In the eastern SCS, peak rainy season occurs in August at all latitudes from 7°N to 21°N with a miximum occurring around 13°N. The peak rainy season matches peak southwesterly monsoon. In the western SCS, on the other hand, the peak rainy season takes place toward the end of the summer monsoon season: It varies from August at the northmost latitude and progressively later up to November-December at 5°N.

The seasonal distribution of rainfall also displays considerable latitudinal variations. Figure 2 displays seasonal variation of HRC, surface winds, and SST at three different latitude bands. In the southern part of SCS around 8°N, the seasonal distribution of rainfall, unlike typical monsoon climate, exhibits a prominent semi-annual cycle with a major peak in

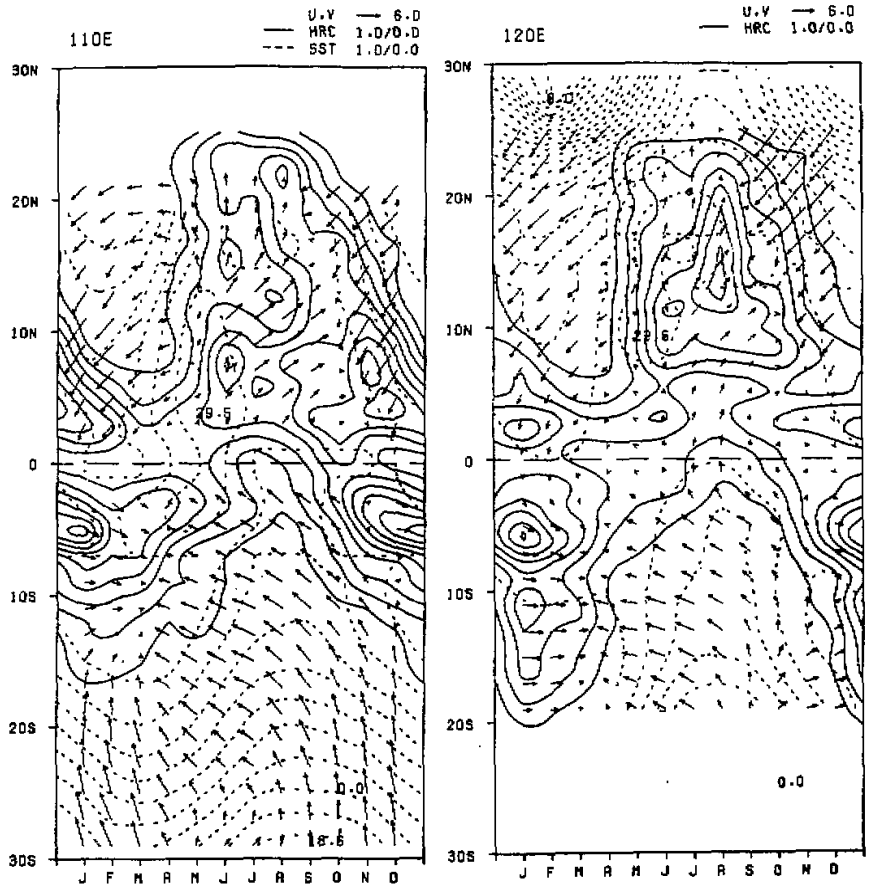

Fig. 1. Climatological monthly mean surface winds, SST (Sea Surface Temperature), and monthly frequency of HRC (Highly Reflective Clouds) along 110°E (left panel) and 120°E (right panel). Contour intervals for HRC and SST are, respectively, 1°C and 1 day per month.

November and a minor peak in June. The two peaks concur with summer monsoon withdrawal and onset, respectively. The heavy rainfall accompanied by withdrawal of summer monsoon is associated with cold air outbreak which penetrates deep into the tropics and enhanced by blocking effects of island (Borneo) topography. In the central SCS around 14°N, HRC frequency displays remarkable east–west gradient: *the HRC frequency off the coast of Vietnam in only about one third of that off the coast of Luzon* (Fig. 2b). The dry climate near the coast of Indo–China peninsula results primarily from the relatively low SST in situ which is caused by southwest monsoon–induced coastal upwelling. The contrast in rainfall implies a strong upward motion near Philippine and relatively sinking near the coast of Indo–China peninsula.

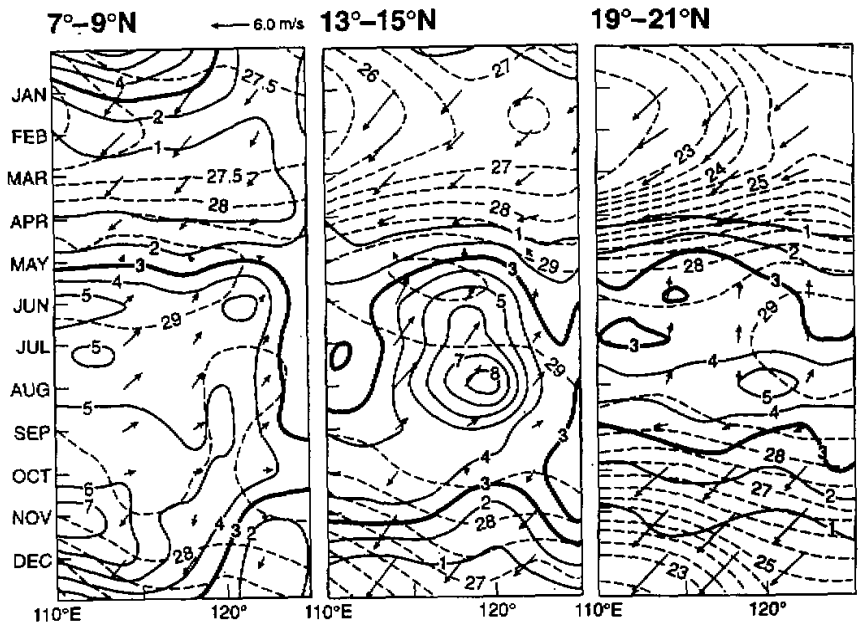

Fig. 2. Same as in Fig. 1 except that the profiles are along 8°N, 14°N, and 20°N, respectively.

The relatively dry zone along the coast of Indo-China peninsula provides a natural boundary between the Indian and the western North Pacific summer monsoons. In view of the relative dryness in the western SCS, it is necessary to perform high resolution, meticulous computations to assess the role of SCS in maintaining Asian monsoon as a heat source. It is probably inadequate to claim the entire SCS area as a summer heat source region.

IV. PROMINENT MONSOON SINGULARITIES

The evolution of mean monsoon is not only associated with climatological annual cycle, but also contains a significant subseasonal component. Figure 3 presents climatological pentad mean OLR averaged over the central SCS (7.5–17.5°N, 112.5–117.5°E) and 850 hPa zonal wind averaged over the southern-central SCS (2.5–12.5°N, 107.5–117.5°E). It is evident that the annual variations of the OLR and 850 hPa winds averaged over these large areas consist of a smoothed annual cycle (denoted by the first three Fourier harmonics) and a 20–70 days component (CISO) with considerable amplitude during boreal summer from May to September (Fig. 3c). Notice that, the OLR and 850 hPa zonal wind CISO are derived from two independent datasets. Yet, they are highly coherent: The westerly anomalies (departure from climatological annual cycle) are negatively correlated with OLR anomalies truly well from May to October. This relationship can be readily explained in terms of a response of tropical atmosphere to convective heating (Gill, 1980): heating induces westerlies to its south and southwest due to Rossby wave dispersion. The coherency between OLR and winds derived from two independent observations adds confidence to the existence of CISO. Physically, CISO results from phase-locking of transient intraseasonal oscillation to annual cycle. It reflects the effect of regulation of annual cycle on transient ISOs.

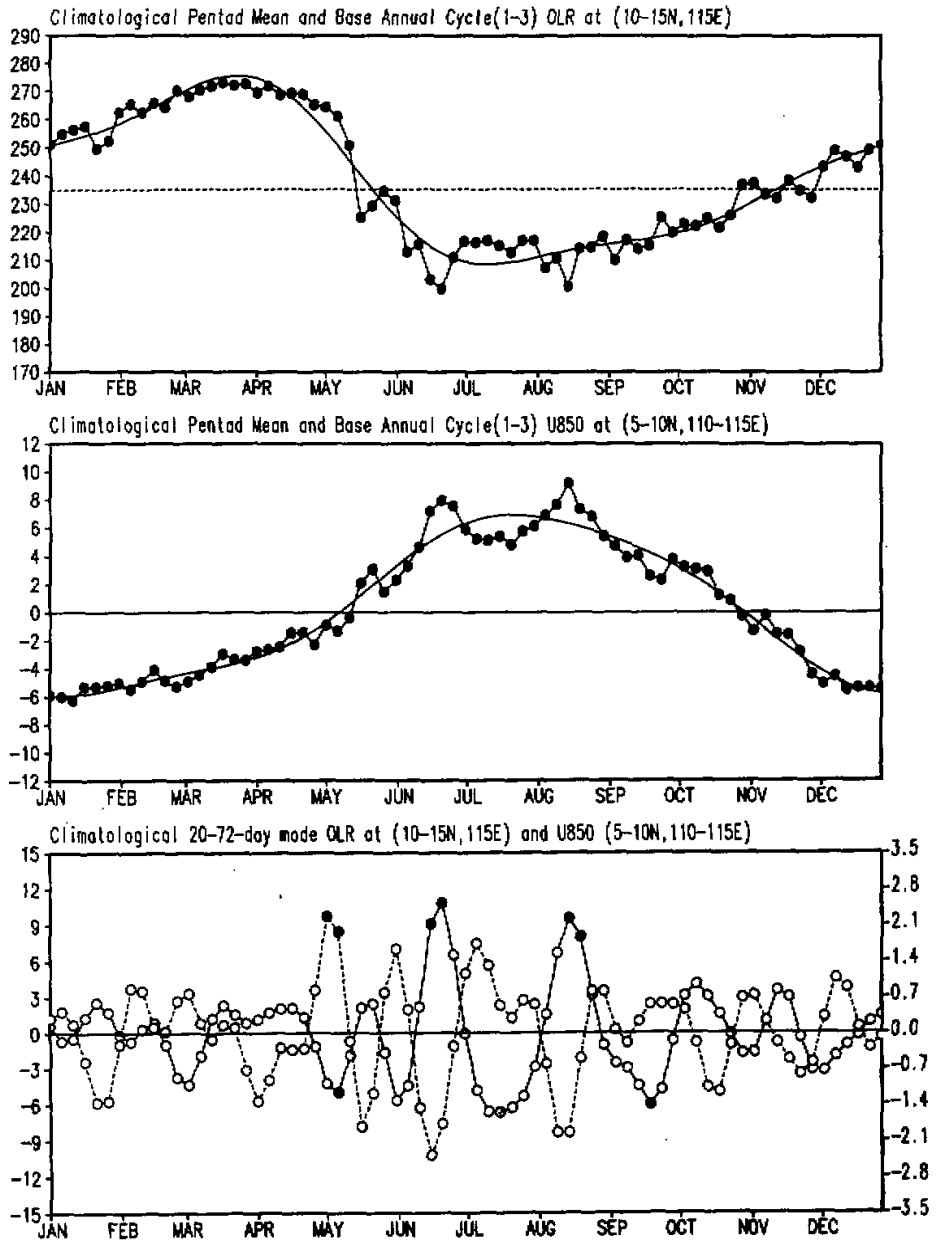

Fig.3 (a) Climatological pentad mean OLR averaged over (7.5–17.5°N, 112.5–117.5°E) (upper panel), (b) climatological pentad mean 850 hPa zonal wind speed averaged over the region (2.5–12.5°N, 107.5–117.5°E) (middle panel), and (c) the corresponding climatological intraseasonal oscillation (CISO) in OLR (dashed) and 850 hPa zonal wind (solid) shown in (a) and (b). The smoothed curves in (a) and (b) represent the base annual cycle which consists of the first three Fourier harmonics of the climatological pentad mean series. The solids in (c) indicate the pentads at which the 850 hPa zonal wind and OLR exhibit a singularity detected by t-test at the 95% confidence level.

Statistically significant extrema of CISO are referred to as monsoon singularities— the events that occur at a fixed pentad of the calendar year on a regular basis (Wang and Xu, 1997). The statistic significance of the monsoon singularities has been tested using both the t–test and sign–test described in Section 2.

The major summer monsoon singularities over SCS, as detected from 850 hPa zonal wind component include (I) the pre–onset easterly extreme at P26 (May 6–10), (ii) the westerly extreme at P34–P35 (June 16–24) following the onset of the western North Pacific summer monsoon (WNPSM), (iii) the anomalous easterly extreme at P40 (July 16–20), (iv) the westerly extreme at P46–P47 (August 14–22) during the peak WNPSM, and (v) the easterly extreme at P53 (September 18–22). These singularities are all statistically significant at 95% confidence level by t–test.

Note that *the singularities in OLR field are much less pronounced than those in the low–level monsoon westerlies* (Fig. 3c). The only significant singularity in OLR time series, which passes the t–test at 95% confidence level, is the pre–onset dry at P25–26 (May 1–10). This dry singularity is very robust. The frequency of occurrence of a positive OLR CISO at these two pentads was 15 / 17 during 1975–1992.

V. PRONOUNCED SUBSEASONAL CYCLES

From May to October, *the subseasonal variation of SCSSM is dominated by four CISO cycles and associated singularities* (Fig. 3c). Climatological active and break monsoons occur alternatively. There are four major easterly and dry phases peaking at P26 (May 6–10), P31 (May 31–June 4), P39 (July 10–14), and P53 (September 18–24), respectively (Fig. 3c). They correspond to the pre–onset dry, the first, second, and the last climatological break monsoons, respectively. There are four major southwesterly surges and the wet spells: The first at P28–29 (May 16–25) marks the SCS summer monsoon onset; the second westerly burst at P34–P35 (June 16–24) follows the western North Pacific summer monsoon (WNPSM) onset; the third westerly burst at P46–P47 (Aug. 14–23) is concurrent with the peak monsoon rain in the western North Pacific; and the fourth wet extreme at P59 (Oct. 18–23) represents the last climatological active monsoon in SCS and the western North Pacific.

The subseasonal variation of SCS summer monsoon is not a local phenomenon. It is intimately linked to the large–scale CISO cycles in the Northern Hemisphere summer monsoon domain as documented in detail by Wang and Xu (1997). The monsoon singularities over SCS are primarily tied to the CISOs propagating from the south and from the east.

From May to July, the subseasonal variation over SCS is primarily associated with a poleward migration of CISO anomalies (both in OLR and 850 hPa southwesterlies) from the equatorial maritime continent to 25°N (Fig. 4). Inspection of intraseasonal oscillation in each individual year reveals that, during about two thirds of the years between 1975 and 1994, there exist systematic northward propagation of transient ISO with a mean propagation speed of about 1.5 m / s (figure not shown). *From July to September, on the other hand, the subseasonal variation over SCS is intimately related to westward propagating CISOs from the western North Pacific near the dateline to Indo–China Peninsula* (Fig. 5). This is particularly evident in OLR field. From July to September, the westerward propagating ISO is a dominant mode along 10–20°N in the western North Pacific (Nitta, 1987; Wang and Rui, 1990). During that period, the westward propagation of transient ISOs appears to be more systematic than the northward propagation occurring in May and June. An example was given in the

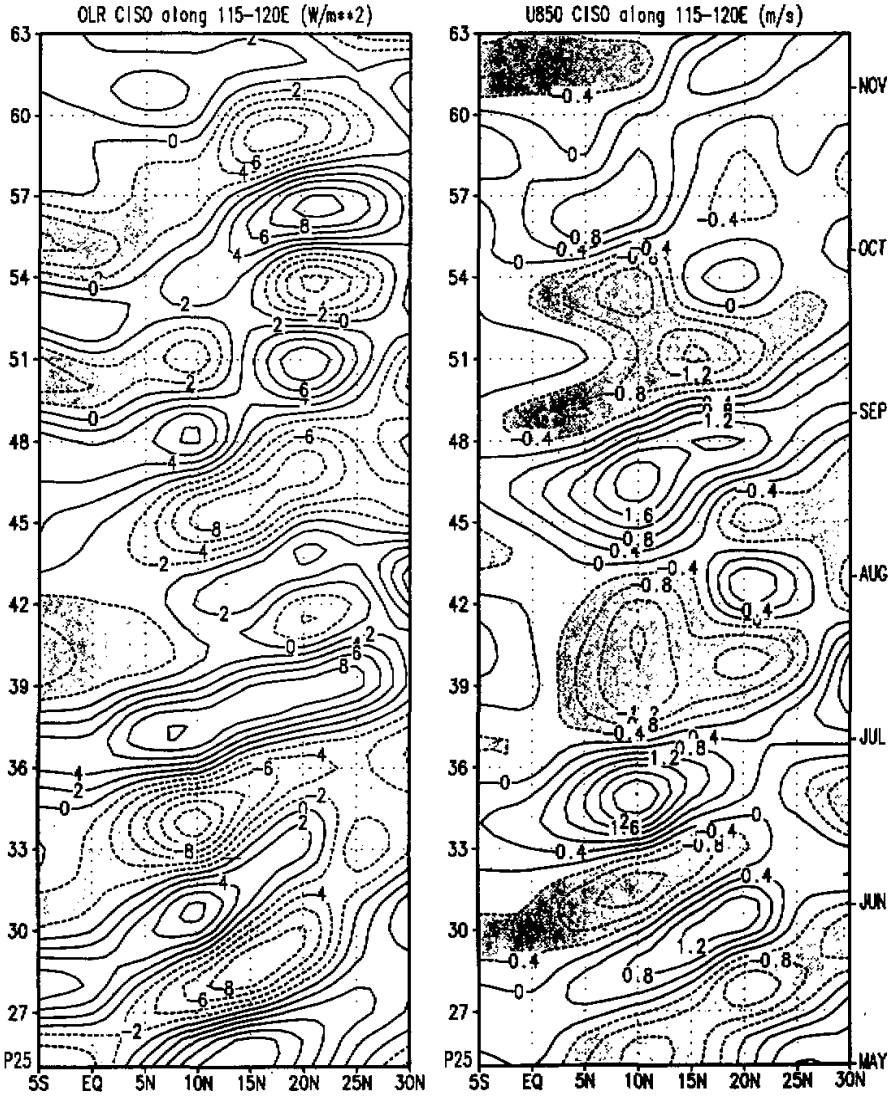

Fig. 4. Latitude–time diagrams displaying the northward propagation of the OLR (left panel) and 850 hPa zonal wind (right panel) climatological intraseasonal oscillation (CISO) along 115–120°E from Julian pentad 25 to pentad 63.

Figure 1 of Wang and Xie (1996). These transient ISOs occur in approximately the same period of the year in accord with seasonal march of the general circulation systems. This confirms the notion that the CISO is a result of the phase–locking of transient ISOs to seasonal march.

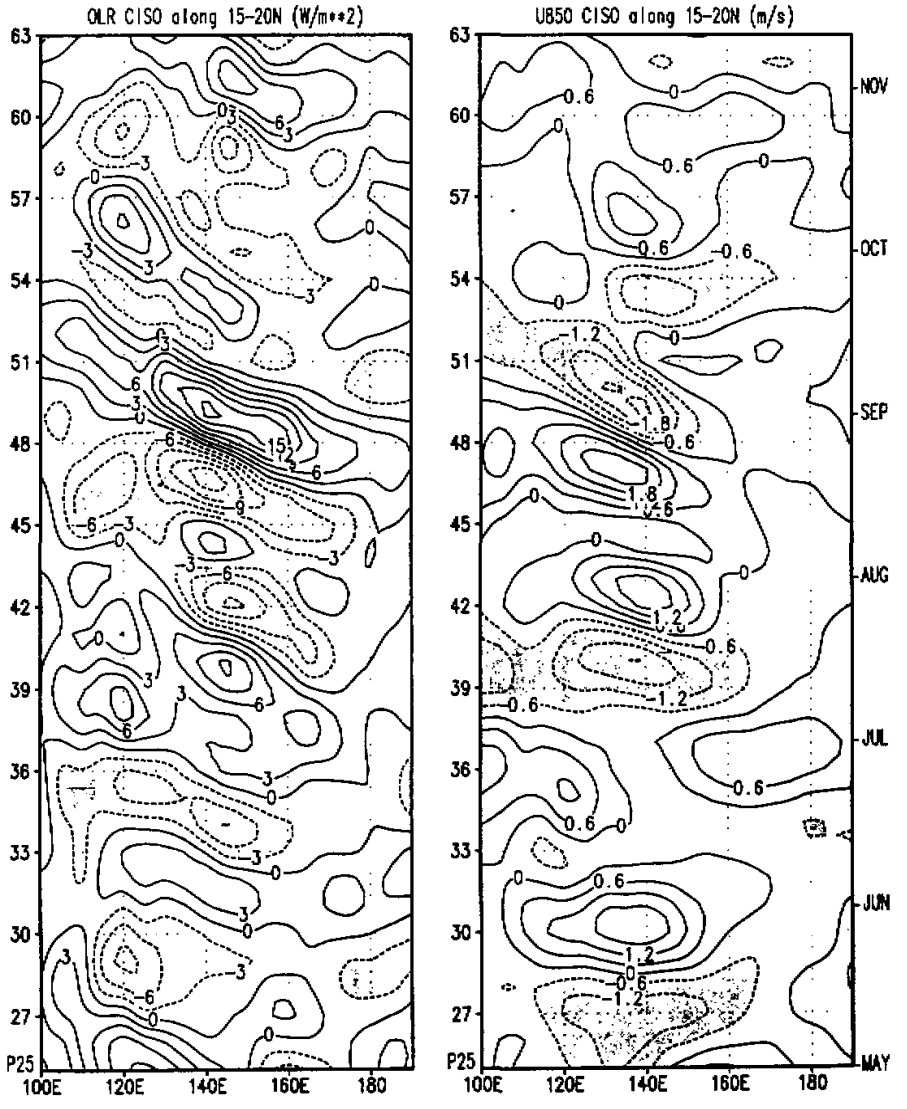

Fig. 5. Longitude–time diagrams displaying westward propagation of the OLR (left panel) and 850 hPa zonal wind (right panel) climatological intraseasonal oscillation (CISO) along 15–20°N from Julian pentad 25 to pentad 63.

VI. THE OUTBUST OF MONSOON RAIN IN MID-MAY

The onset of SCSSM is characterized by a sudden shift wind direction from southeasterlies to southwesterlies over central SCS and by an outburst of monsoon rainy season in central–northern SCS. Climatologically, they occur simultaneously and abruptly at P28 (May 16–20) (Figs. 6a,b). This process is nearly simultaneous with the development of

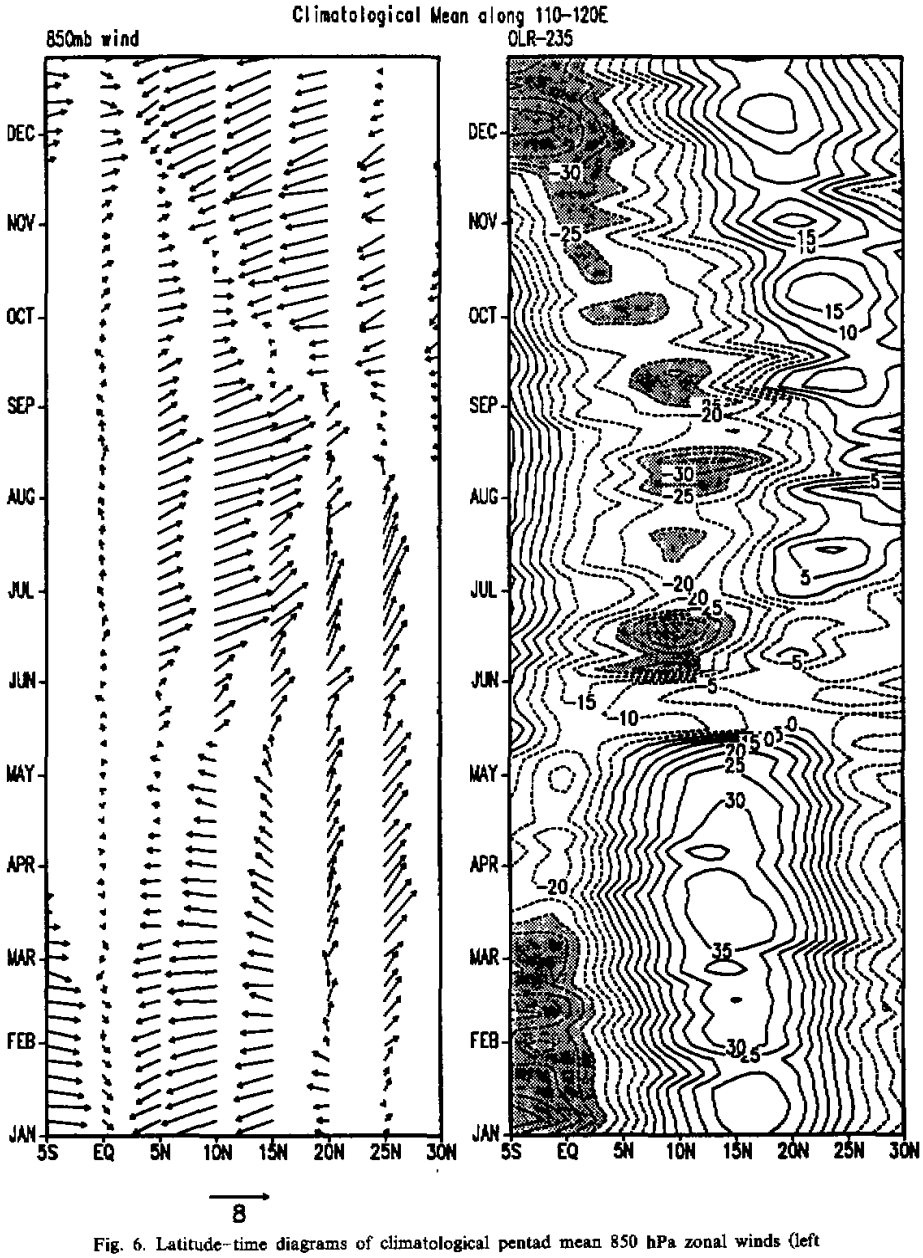

Fig. 6. Latitude–time diagrams of climatological pentad mean 850 hPa zonal winds (left panel) and the OLR departure from 235 W / m^2 (right panel) along 110–120°E. The OLR contour interval is 5 W / m^2.

heavy rain along the Southern coast of mainland China. Taiwan, and Akinawa, starting the first quasi-stationary stage of the East Asian subtropical monsoon rain (Tao and Chen,

1987; Ding, 1992; Tanaka, 1992).

The start of the monsoon rainy season over SCS is remarkably abrupt: From P27 to P28, the pentad mean OLR drastically decreases by about 30 W / m^2 at (15°N, 115°E)(Fig. 6a). The pentad mean OLR averaged over a large area (10–20°N, 110–120°E) drops 16 W / m^2 from 245 W / m^2 at P27 to 229 W / m^2 at P28. The corresponding pentad mean rainfall exceeds about 8 mm / day at P28. The establishment of southwest monsoon is also spectacularly fast: *From P27 to P28, the pentad mean 850 hPa zonal wind averaged over the south and central SCS suddenly increases by 3.2 m / s* from 1.3 m / s easterlies to 1.9 m / s westerlies (Fig. 6b).

Accompanying the hasty changes in winds and convection, the 850 hPa vorticity field over the northern SCS experiences a quick switch from anticyclonic to cyclonic. This can be clearly seen from 850 hPa winds along 115°E from 10°N to 20°N (Fig. 6a). At P27, the wind changes northward from easterly to strong southwesterly, implying that the northern SCS is under control of anticyclonic flows associated with western Pacific subtropical high. In sharp contrast, at P28 winds change northward from southwesterlies to southerlies, implying that the northern SCS is dominated by cyclonic flows associated with a monsoon trough which extends from Indo-China Peninsula to South of Philippines. This is well in accord with Matsumoto's (1992) results which were displayed using climatological pentad mean map derived for a shorter period of 1980–1987.

It should be pointed out that *the abrupt regime-transition in Mid-May is attributed to not only the CISO but also the asymmetric transition in the annual cycle.* Figure 3a shows that the smoothed annual cycle displays a much sharper gradient in May compared to that in October. The pentad mean OLR decreases by 35 W / m^2 in May while only increases by 9 W / m^2 in October. *Superposed on this rapid May transition in annual cycle is a keen mid-May transition in CISO of the same sense, which makes the outburst of climatological monsoon rain at P28.*

VII. THE SUBSTANTIAL YEAR-TO-YEAR VARIABILITY IN PENTAD MEAN OLR

In contrast to the extreme phases of CISO, the transition phase of CISO result from large year-to-year variability of the transient ISOs. Since a failure monsoon rainy season is often associated with missing a major active monsoon spell or with a prolonged break monsoon, study of the interannual variation of active / break monsoon cycle (subseasonal variation of monsoon) is of fundamental importance. The transition phases of CISO provide a useful clue to searching for subseasonal structure of the year-to-year monsoon variability.

The OLR over SCS exhibits considerably larger interannual variations on intraseasonal time scales than those in the other Northern Hemisphere tropical monsoon regions: the Bay of Bengal and Philippine Sea. This can be seen from Fig. 7 which illustrates variabilities of the two components of ISO: The amplitude of CISO which is the component phase-locked to annual cycle (the light shadings) and the standard deviation of the ISO component that is due to interannual variation (the dark shading). Over SCS, the summer (May–October) mean magnitude of CISO, A, is 4.4 W / m^2 which is smaller than those over the Bay of Bengal (5.2 W / m^2) and the Philippine Sea (5.8 W / m^2). On the other hand, the standard deviation of pentad mean OLR anomalies, S, over SCS (22 W / m^2) is larger than those over the Bay of Bengal (16.9 W / m^2) and the Philippine Sea (19.8 W / m^2). The ratio, S / A, which measures the relative magnitude of the interannual variation vs. the phase-locking component, over SCS (5.04) is substantially larger than the corresponding counterparts over the Bay of Bengal (3.25) and the Philippine Sea (3.43). More detailed analysis indicates that the intraseasonal

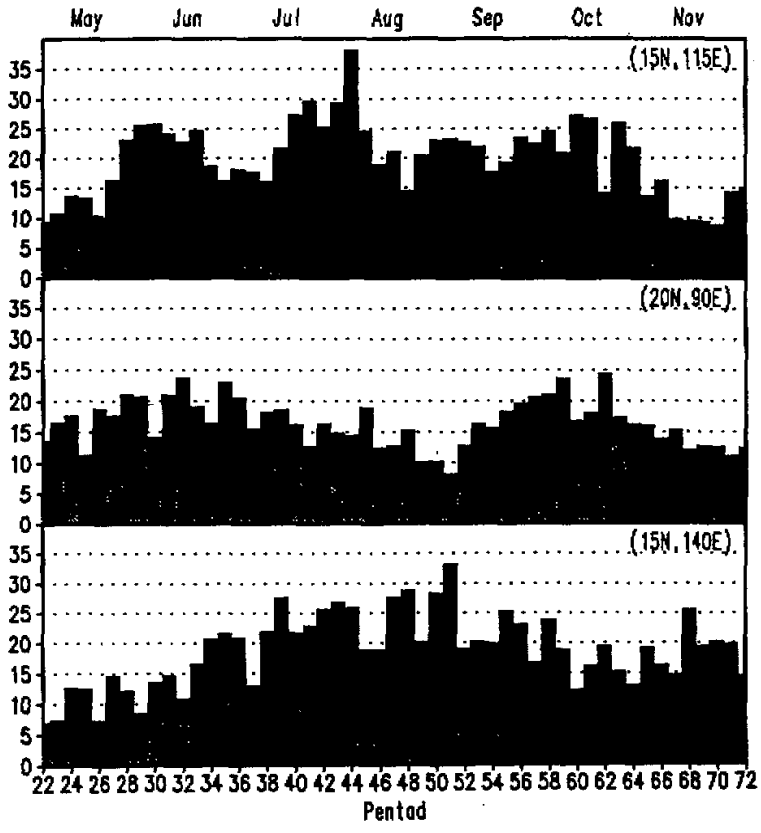

Fig. 7. Histograms showing the magitude of OLR CISO (light shadings) and the standard deviation of the transient ISO at each pentad for three different regions: the South China Sea (upper), the Bay of Bengal (middle), and the Philippine Sea (lower). The ordinate is in units of W/m^2.

oscillations over SCS are notably variable from year to year in their amplitude, periodicity, and phases.

VIII. BI-MODAL INTERANNUAL VARIATION IN MONSOON ONSET

Although the pre-onset dry (P25-26) is a monsoon singularity (remarkably regular occurrence from year to year), the SCSSM onset at P28 is not. The year-to-year variation of OLR at P28 is substantially larger than CISO amplitude (Fig. 7a). In fact, the beginning of monsoon rainy season displays considerable interannual variation. To demonstrate this, we need to define the onset pentad for each individual year.

It is not trivial to determine summer monsoon onset for individual years, although the climatological monsoon onset over SCS can be determined without any ambiguity (Fig. 3). To be objective, we propose the following criteria based on both pentad mean OLR and 850 hPa zonal wind component.

The beginning of the monsoon rainy season is defined using pentad mean OLR series av-

eraged for the central–northern SCS region (7.5–22.5°N, 110–120°E). The onset pentad must satisfy two conditions: (I) the pentad mean OLR is below 235 W / m^2 and (ii) the mean OLR in the subsequent six pentads (including the ouset pentad) is also below 235 W / m^2.

The onset of southwesterly monsoon is defined using 850 hPa pentad mean zonal wind averaged over the central–southern SCS region (2.5–12.5°N, 110–120°E). The onset pentad must satisfy the following two criteria: (I) the pentad mean u_{850} exceeds 0.5 m / s and (ii) the mean u_{850} in the subsequent six pentads (including the onset pentad) also exceeds 0.5 m / s.

The onset pentads of monsoon rain and southwesterlies for each year determined by the above criteria are listed in Table 1. The start of rainy season basically concurs with the establishment of steady southwest monsoon. However, during 1987, 1991, and 1992 they differ by two pentads (Table 1). We, therefore, define the SCSSM onset by the starting pentad of the rainy season except when the onset of southwest monsoon differs from the start of rainy season by two or more pentads. In the latter exceptional situation, the SCSSM onset can be defined by the averaged date of the two (values are given in the last line of Table 1).

Table 1. List of the Julian pentads at which (a) the SCS rainy season begins (the OLR), (b) the southwesterly monsoon establishes in the southern–central SCS (the u_{850}), and (c) the onset of the SCS summer monsoon for each individual year and for climatological mean. The precise definitions of the items (a), (b) and (c) are referred to the next

Year	75	76	77	79	80	81	82'	83	84	85	86	87	88	89	90	91	92	mean
OLR	31	29	34	27	28	27	28	29	24	30	27	31	29	28	27	31	30	28
u_{850}	--	--	--	27	27	27	28	29	24	30	27	33	29	28	28	33	28	28
Onset	(31)	(29)	(34)	27	28	27	28	29	24	30	27	32	29	28	27	32	29	28

During the period of 1975–1992, the earliest SCS rainy season starts in late April (P24: April 26–30) (1984), while the latest starts in mid–June (P34: June 14–18) (1977). This is a notably large time window. However, about 65% (11 / 17) of the years, the summer monsoon starts in between P27 and P29 (May 11–May 25). Among the other six abnormal onset years, the majorities (5 / 6) are late onsets (from P30 to P34, or May 25–June 18) which occur in 1975, 1977, 1985, 1987, and 1991. There is no obvious and robust connection between SCSSM onset date and occurrence of ENSO.

It appears to be evident that the interannual variation of the SCSSM onset takes two modes: a normal mode (the onset occurs around climatological mean date—during P27–P29) and a delayed mode (the onset occurs during P30–34, most likely in early June). The bimodal behavior has to do with the existence of the strong monsoon singularity in early May. The presence of conspicuous pre–monsoon dry singularity at P25–26 (May 1–10) strongly prevents early onset (1984 is an exceptional case) and constrains monsoon onset in majority (about two thirds) of the years to the ensuing three pentads (P27–29, or May 11–25). The abnormal onset is, therefore, dominated by a delayed mode. During the delayed onset year, the wet spells which follow the early–May dry singularity are normally weak.

IX. THE RED SPECTRUM OF THE TRANSIENT DISTURBANCES

In the literature, the SCS disturbances were described to cover a broad range of time scales including short convective scale, diurnal cycle, 3–5 day mid–troposphere cyclone and monsoon depression, tropical cyclones, and intraseasonal oscillations with 10–20 day and 30–60 day periodicities. the detailed temporal structure and spectral properties of SCS disturbances are not well documented.

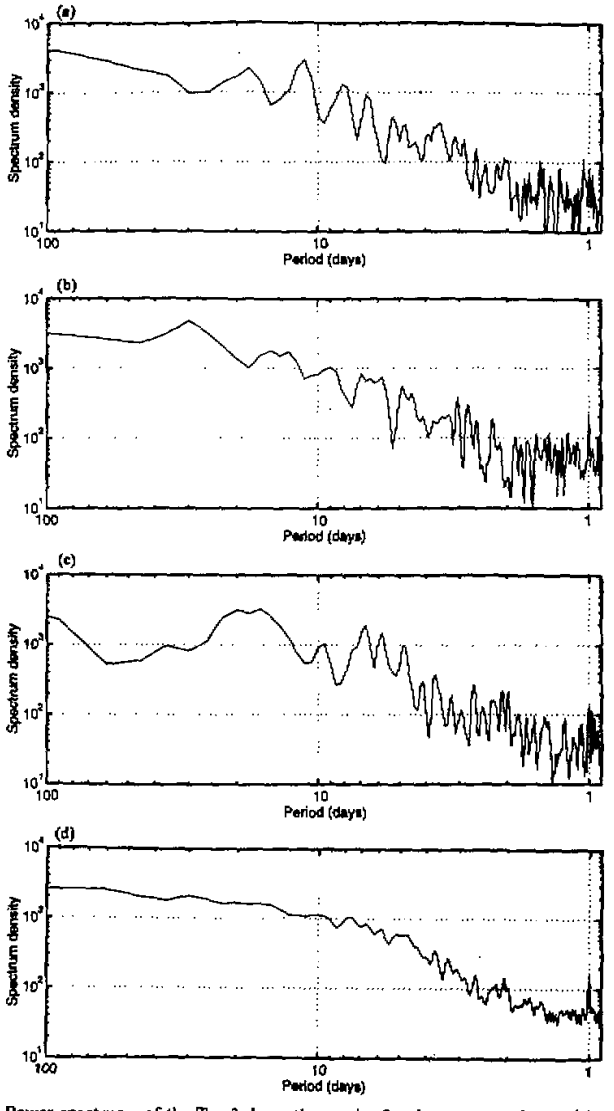

Fig. 8. Power spectrums of the T_{BB} 3-hour time series for the summer of 1991 (a), 1992 (b), 1993 (c), and for a 9-year mean spectrum (d) at (15°N, 115°E).

Spectrum analysis of three-hourly time series of T_{BB} was performed for each year from 1979 to 1992 to infer spectral properties of the deep convection and rainfall. Figure 8 shows spectra for three individual summers and a climatological mean spectrum averaged from the spectra of each individual summer at (15°N, 115°E). The spectrum for each individual summer appears to show, to some degrees, a concentration of energy on one or several preferred time scales. For instance, the 11-day peak in 1991, the 30-day peak in 1992, and the 7-day and 16-20 day peaks in 1992. In other years, spectral peaks are centered at a variety of other

time scales: 2 days, 5 days, 7–10 days, or 15–20 days, etc.. *The mean spectrum, however, clearly denies the significance of any of these peaks that appear to be evident during individual years.*

Figure 8 suggests that *the mean spectrum of deep convection activity over northern SCS is essentially red beyond diurnal cycle.* It fits well into a Markov chain model. No dominant time scale is preferred for the synoptic and intraseasonal disturbances. This is probably an unexpected result. There are two possible causes for this red power spectrum. First, the SCS region is under random influences of various types of disturbances which have diverse time scales. These disturbances invade SCS at a random basis (in climatological sense) from adjacent regions such as from East Asia subtropical front, from the western Pacific monsoon trough, and from the equatorial regions, sometimes they are generated in-situ. Second, the synoptic to intraseasonal variability over SCS is nonstationary with notably variable periodicity from year to year. This could result in a red mean spectrum.

X. SUMMARY

A number of distinctive features in the temporal structure of the SCSSM have been revealed and demonstrated in this study. These features are summarized as follows:

- The lower tropospheric monsoon flows exhibit pronounced singularities. Four robust singularities are identified in 850 hPa winds: the pre-onset southeasterly trade wind surge at P26 (May 6–10), the southwesterly bursts at P34–P35 (June 15–24) and P46–47 (August 14–23), and the anomalous easterly surge at P40 (July 10–14) and P53 (September 18–22).
- The evolution of SCSSM displays four prominent subseasonal cycles—the alternative occurrences of climatological active and break monsoons (Fig. 3c). These prominent subseasonal cycles of the SCSSM are primarily linked to the variations over the Maritime Continent by northward propagation of climatological intraseasonal oscillation (CISO) during May–July and linked to the variations over the western North Pacific by westward propagation of CISO during August and September.
- The seasonal transitions of SCS monsoon are remarkably asymmetric: The onset of summer monsoon is nearly simultaneous across the entire latitudinal extent of SCS, whereas the withdrawal is progressively later equatorward, taking about four months (Fig. 1).
- The onset of mean SCSSM is an extremely abrupt transition in mid-May from P27 (May 11–15) to P28 (May 16–20) (Fig. 6). The onset is characterized by (a) an outburst of monsoon rain in central-northern SCS (7.5–22.5°N, 110–120°E): the climatological pentad mean OLR averaged over this large region dramatically decreases by 16 W / m^2 and (b) a sudden shift of wind direction from southeasterlies to southwesterlies over southern-central SCS (2.5–12.5°N, 110–120°E): the climatological pentad mean 850 hPa zonal wind averaged over this region suddenly increases by 3.2 m / s from 1.3 m / s easterlies to 1.9 m / s westerlies.
- The convection and rainfall as revealed from OLR display considerably larger year-to-year variability over SCS compared to other regions of the Northern Hemisphere tropical monsoon such as over the Bay of Bengal and the Philippine Sea (Fig. 7).
- The interannual variation of monsoon onset exhibits two dominant modes: a normal and a delayed mode. The presence of conspicuous pre-monsoon dry singularity at P25–26 (May 1–10) strongly constrains the monsoon onset to the ensuing three pentads (P27–29, or May 11–25) for about two thirds of the years (Table 1). The abnormal onset is dominated by a delayed mode (P30–34). The delayed onset does not appear to be related to ENSO cycle.
- The mean spectrum of deep convection over northern SCS is essentially red beyond the diurnal cycle which is well fitted into a Markov chain model (Fig. 8d). No preferred periodicity was found on synoptic to intraseasonal time scales in climatological mean sense.

This means that the prevailing weather rhythm changes from year to year and is highly nonstationary.

• There exists a large east–west gradient of rainfall in the central SCS (Fig. 2). The formation of the dry zone along the coast of Indo–China peninsula results from the monsoon–ocean interaction: the southwesterly monsoon induces coastal upwelling and decreases in SST off the coast of Vietnam which in turn suppresses deep convection.

The results presented here are preliminary. In view of the limited data coverage and sample size and the limited fields examined, more comprehensive data analyses are also needed concerning the peculiar nature of the SCSSM. In spite of the limitations, the features revealed in this study are believed to be qualitatively robust.

We have discussed possible causes that are responsible for some of the features listed above, e.g., the possible causes for the east–west contrast in rainfall, the lack of dominant oscillation period in the mean T_{BB} spectrum, the bi–modal behavior of the monsoon onset, and the sharp transition in mid–May. Further investigations are needed to explain other distinctive features. In particular, the following questions should be addressed:

• Why is the onset of SCSSM nearly simultaneous over the large latitudinal extent of SCS while the withdrawal occurs progressively later equatoward?

• What causes the pronounced monsoon wind singularities over SCS? Why does CISO ttend to propagate northward in early summer while westward in late summer?

• Why does the deep convection over SCS experience the largest year–to–year variability compared to other tropical monsoon regions?

• Why the mean spectrum of OLR in northern SCS is essentially red beyond the diurnal cycle?

• What determines the regularity of the pre–onset dry and the delayed monsoon onset?

• What causes the sharpest mid–May transition over SCS in both the annual cycle and CISO component?

Some of the conclusions reached in this study may differ from those obtained by previous studies. It is our hope that the points raised here will be of some use for the design of the SCSMEX field program and stimulate further observational and model studies of the coupled Asian Monsoon System.

This study is supported by the Climate Dynamics Program of NSF under grant number ATM–9400759 and the Marine Meteorology Program of ONR under the grant No N00014–96–1–0796. The authors thanks Mrs. Z. Fang and Y. Wang and Ms. H. Teng for preparation of part of the data and figures. This is the School of Ocean and Earth Science and Technology publication No. XXXX.

REFERENCES

Ding, Y.–H. (1992), Summer monsoon rainfall in China, *J. Meteor. Soc. Japan*, **70**: 373–396.

Garcia, O. (1985), *Atlas of Highly Reflective Clouds for the Global Tropics: 1971–1983*, U.S. Dept. of Commerce, NOAA, Environmental Research Lab., 365pp.

Gill, A.E. (1980), Some simple solutions for heat induced tropical circulation, *Quart. J. Royal. Meteor. Soc.*, **106**: 447–463.

Huang, R.H., and W.J. Li (1988), The effect of heat source anomaly over the tropical western Pacific during summer, *Chinese J. Atmos. Sci.*, (Special issue).

Huang, Z. and S.Y. Tao (1992), Diagnostic study of the bursting processes of Asian summer monsoon in 1983, *Acta Meteor. Sinica*, **50**: 210–217 (in Chinese).

Kilonsky, B.J. and C.S. Ramage (1976), A technique for estimating tropical open–ocean rainfall from satellite ob-

servations, *J. Appl. Meteor.* **15:** 972–976.

Krishnamurti, T.N. (1985), Summer monsoon experiment, A review, *Mon. Wea. Rev.*, **113:** 1590–1626.

Lau, K.-M. and L. Peng (1992), Dynamics of atmospheric teleconnection during northern summer, *J. Atmos. Sci.*, **5:** 140–158.

Lau, K.-M., and S. Yang (1997), Climatology and interannual variability of Southeast Asian summer monsoon, *Advances in Atmospheric Sciences*, **14(2):** 141–162.

Matsumoto, J. (1992), Climate over Asian and Australian monsoon regions, the University of Tokyo Project No, 03212–103.

Marissey, M.L. (1986), A statistical analysis of the relationships among rainfall, outgoing longwave radiation and the moisture budget during January– March 1979, *Mon. Wea. Rev.*, **114:** 931–994.

Motell, C.E., and B.C. Weare (1987), Estimating tropical Pacific rainfall using digital satellite data, *J. Climate Appl. Meteor.*, **26:** 1436–1446.

Nitta, T. (1987), Convective activities in the tropical western Pacific and their impact on the Northern Hemisphere summer circulation, *J. Meteor. Soc. Japan*, **41:** 373–390.

Sadler, J.C., M.A. Lander, A.M. Hori and L.K. Oda (1987), Tropical marine climatic atlas, Vol. 2, Pacific Ocean, Report UHMET 87–02, Department of Meteorology, University of Hawaii, Honolulu, HI 96822, 27pp.

Tao, S.Y. and L. Chen (1987), A review of recent research on the East Asian summer monsoon in China, in *Monsoon Meteorology*, C.P. Chang and T.N. Krishnamurti eds., Oxford University Press, 60–92.

Tomita, T. and T. Yasunari (1996), Role of northeast winter monsoon on the biennial oscillation of the ENSO / monsoon system, *J. Met. Soc. Japan*, **74:** 399–413.

Wang, B. (1994), Climatic regimes of tropical convection and rainfall, *J. Climate*, **7:** 1109–1118.

Wang, B. and H. Rui (1990), Synoptic climatology of transient tropical intraseasonal convection anomalies: 1975–1985, *Meteor. Atmos. Phys.*, **44:** 43–62.

Wang, B. and X. Xie (1996), On the impacts of Northern Hemisphere summer monsoon on intraseasonal oscillation, *J. Atmos. Sci.*.

Wang, B. and X. Xu (1997), Northern Hemisphere summer monsoon singularities and climatological intraseasonal oscillation, *J. Climate*, to be published.

Webster, P.J. and S. Yang (1992), Monsoon and ENSO: Selectively interactive systems, *Quart. J. R. Meteorol. Soc.*, **118:** 877–926.

Yasunari, T. (1991), "The monsoon year"—a new concept of the climatic year in the tropics, *Bull. Am. Meteor. Soc.*, **72:** 1331–1338.

Zhu, Q., J. He and P. Wang (1986), A study of the circulation differences between East Asian and Indian summer monsoons with their interaction, *Advances in Atmos. Sci.*, **3:** 466–477.